Prediction of intramuscular fat levels in Texel lamb loins using X-ray computed tomography scanning

Clelland, N; Bunger, L; McLean, KA; Conington, JE; Maltin, C; Knott, S; Lambe, NR

Published in:
Meat Science

DOI:
10.1016/j.meatsci.2014.06.004

Print publication: 01/01/2014

Document Version
Peer reviewed version

Prediction of intramuscular fat levels in Texel lamb loins using x-ray computed tomography scanning

N. Clelland[a*], L. Bunger[a], K.A.McLean[a], J. Conington[a], C. Maltin[cd], S. Knott[b], and N.R. Lambe[a]

[a]Animal Breeding and Genetics, Animal and Veterinary Sciences group, Scotland's Rural College (SRUC), West Mains Road, Edinburgh, EH9 3JG, UK

[b]Institute of Evolutionary Biology, School of Biological Sciences, University of Edinburgh, Ashworth Laboratories, West Mains Road, Edinburgh, EH9 3JT, UK.

[c]Quality Meat Scotland (QMS), Rural centre, West mains, Ingliston Newbridge, EH28 8NZ

[d]Present address: Biomics Ltd, Inverurie, Aberdeenshire AB51 0LE

Corresponding author: Neil Clelland, Scotland's Rural College (SRUC), Roslin Institute Building, Edinburgh, EH25 9RG, UK. Tel: +44 131 651 9293. Email: neil.clelland@sruc.ac.uk

Keywords: x-ray computed tomography, lamb, meat quality, intramuscular fat.

Abstract

For the consumer, tenderness, juiciness and flavour are often described as most important for meat eating quality, all of which have a close association with intramuscular fat (IMF).

X-ray computed tomography (CT) can measure fat, muscle and bone volumes and weights, *in vivo* in sheep and CT predictions of carcass composition have been used in UK sheep breeding programmes over the last few decades. This study aimed to determine the most accurate combination of CT variables to predict IMF percentage of *M. Longissimus lumborum* in Texel lambs.

As expected, predicted carcass fat alone accounted for a moderate amount of the variation ($R^2 = 0.51$) in IMF. Prediction accuracies were significantly improved ($R^2 > 0.65$) using information on fat and muscle densities measured from three CT reference scans, showing that CT can provide an accurate prediction of IMF in the loin of purebred Texel sheep.

1. Introduction

It is apparent that fat content of meat plays a significant role in the acceptability of major meat quality (MQ) attributes concerning the consumer and for many decades the influence of fat content on the eating quality of meat has been debated. Generally, four major fat depots are recognised in animal carcasses: subcutaneous (under the skin); internal organ associated (surrounding the kidneys and other internal organs); intermuscular (between muscles); and intramuscular (IMF, within the muscle), the latter having the greatest association with meat eating quality (MEQ) (Smith & Carpenter, 1974; Savell & Cross, 1988)

Consumer-driven preference for leaner meat, coupled with the meat processing industry's preference for reduced carcass fat, increased lean meat yield and reduced waste, have led to continued selection for increased lean growth and a reduction in associated carcass fatness. However, IMF (or marbling) and back fat thickness are genetically positively correlated in meat producing species (such as pigs r_g = 0.31) (Sonesson, de Greef & Meuwissen, 1998). Selection practices focussed upon the reduction of subcutaneous fatness has resulted in an associated decrease in IMF content in pigs and in turn has had a negative effect on the palatability of fresh pork meat. A similar story is starting to emerge from the sheep industry (Pannier, Pethick, Geesink, Ball, Jacob & Gardner, 2014). The genetic correlations between meat quality traits and carcass composition traits have been investigated in sheep, with Lorentzen and Vangen (2011) reporting a moderately high genetic correlation between IMF and dissected fat (kg) (r_g = 0.62). Given the genetic relationship between IMF and carcass fat, and the possible impact on meat (eating) quality traits, it has been recognised that there is a need to investigate the possibility of the selection against this positive correlation, allowing breeders to continue to select for lean meat yield and reduced carcass fatness without compromising aspects of MQ and associated MEQ traits related to IMF levels.

X-ray computed tomography (CT) can measure fat, muscle and bone *in vivo* in sheep and CT predictions of carcass composition have been used in commercial UK sheep breeding programmes over the last few decades (Bunger, Macfarlane, Lambe, Conington, McLean, Moore et al., 2011). Together with ultrasound measures of fat and muscle depth in the loin region, CT measured carcass

fat and muscle weights have contributed substantially to the success of breeding for leaner carcasses and increased lean meat yield (Moore, McLean & Bunger, 2011).

This approach is based broadly on the classification of pixels associated with density values related to the attenuation of x-ray energy as they interact with different tissues, this parameter is measured in Hounsfield units (HU) (Kalender, 2005). Area measurements (mm^2) for different tissues can then be produced from multiple scans taken at optimal anatomical locations across the animal and, from these measurements, weights of each main tissue in the carcass can be estimated, with typical accuracies of 0.99, 0.98 and 0.89 for fat, muscle and bone respectively (Young, Simm & Glasbey, 2001; Macfarlane, Lewis, Emmans, Young & Simm, 2006).

To continue to select for lower carcass fat, whilst avoiding any detrimental effects on MQ via reduced IMF levels, robust and accurate predictions of IMF (preferentially *in vivo*) are needed to inform breeding decisions. CT scanning not only provides information on carcass tissue areas, volumes and weights, but resulting CT muscle density parameters have also been shown to be good predictors of IMF (Karamichou, Richardson, Nute, Mclean & Bishop, 2006; Lambe, McLean, Macfarlane, Johnson, Jopson, Haresign et al., 2010; Macfarlane, Young, Lewis, Emmans & Simm, 2005) .

However, the use of CT parameters related to carcass tissue densities for the prediction of IMF has not been fully investigated. This study aims to investigate the use of a range of CT parameters related to fat and muscle density values (HU) to optimise the prediction of IMF in the loins of Texel lambs *in vivo*.

2. Materials and methods

2.1. Experimental animals

All procedures involving animals were approved by an animal ethics committee at Scotland's Rural College (SRUC) and were performed under United Kingdom Home Office licence following the regulations of the Animals (Scientific Procedures) act 1986.

CT and IMF data were derived from two previously published studies. The first experiment (EXP 1) was conducted over two years (2003-2004) and examined the use of various *in vivo* measurements to predict carcass and meat quality in Texel (n=240) and Scottish Blackface lambs (n=233) (Lambe, Navajas, Schofield, Fisher, Simm, Roehe et al., 2008). The second experiment (EXP 2) was

conducted in 2009 and examined the genotypic effects of the Texel muscling QTL on carcass and meat quality traits in Texel lambs (n=209), which included data from two research farms, in Scotland and Wales (Lambe, Richardson, Macfarlane, Nevison, Haresign, Matika et al., 2011). In the present study, only the data from the research farm in Scotland was used. Both Texel data sets were combined to produce one larger data set (EXP 1&2) consisting of results from the two separate trials over three separate years.

In brief, EXP 1&2 comprises data from pure-bred Texel lambs (n = 377) of both sexes (female and entire males) produced over three separate years (2003, 2004 and 2009). Lambs were reared to weaning as either singles (n = 184), twins (n = 168) or artificially hand reared (n = 25). Mean age at CT was 132 days (SD 21.1, range 91-202 days), with mean live weight 35.32 kg (SD 4.91, range 20-49 kg).

All lambs were lightly sedated (Rompum^{TM}) at a dose of 0.1-0.2 mg xylazine hydrochloride/kg body weight, and were then secured on their backs in a cradle before being CT- scanned pre-slaughter using a Siemens Somatom Esprit scanner at the SRUC-BioSS CT unit in Edinburgh.

2.2. X-ray computed tomography measurements/Image analysis

Two-dimensional (2D) cross-sectional scans (Field of view = 450mm, Resolution = 512x512 pixels) were taken at 3 defined anatomical positions, through the top of the leg at the ischium bone (ISC), the loin at the fifth lumbar vertebra (LV5), and through the chest at the 8th thoracic vertebra (TV8) (Figure 1).

This method of scanning has been defined as 'reference' scanning, optimising the number of images taken while maximising accuracy of prediction for carcass tissue weights, and these specific anatomical sites were derived from previous calibration trials (Bunger et al., 2011). Image analyses were performed to separate carcass from non-carcass tissues (Glasbey & Young, 2002) and the density of each pixel (0.77mm^2) in the carcass portion was allocated to fat, muscle or bone, according to density thresholds using Sheep Tomogram Analysis Routines (STAR) software (Mann, Young, Glasbey & McLean, 2003). Areas (mm^2) and average densities (HU) of each tissue in each 2D image were calculated, as well as standard deviations for the density values of all pixels allocated to each

tissue. A novel soft tissue density (and its standard deviation) was also calculated, combining the information from both fat and muscle tissue densities.

Initial analyses included CT data from all three reference scans. Following this, information from the LV5 scan only was used. Further analyses were then performed identifying a region of interest (ROI) relating to the anatomical position from where the chemically-extracted IMF was measured (*M. Longissimus lumborum*). This involved three levels of precision: (i) identifying the LV5 scan as the ROI; (ii) performing "virtual dissection" of the LV5 image to isolate the ROI to the muscles surrounding the spine, including *M. longissimus*, *M.psoas major* and *M.psoas minor*; (iii) performing virtual dissection of the LV5 image with the ROI restricted to the right side *M. longissimus* muscle (left side of the image) (Figure 2).

Carcass fat, as a measure of subcutaneous and intermuscular fat, was also predicted using a breed-specific prediction equation developed from previous research (Macfarlane et al., 2006):

PR_CFAT (kg) = (-2263 + (LW*80.26) + (ISCFA*0.21) + (LV5FA*0.19) + (TV8FA*0.221))/1000

Where PR_CFAT is the CT predicted weight of subcutaneous and intermuscular fat (kg), LW is live weight at CT scanning, ISCFA is the area of pixels allocated as fat in the scan image taken at the ischium region (mm^2), LV5FA is the area of pixels allocated as fat in the scan image taken at the 5^{th} lumbar vertebra region (mm^2) and TV8FA is the area of pixels allocated as fat in the scan image taken at the 8^{th} thoracic vertebra.

2.3. Slaughter and Meat quality measurements

Mean age at slaughter was 149 days (SD 23.32, range 96 – 234 days), mean live weight at slaughter was 34.81 kg (SD 5.21, range 19.71 – 52.2 kg). The majority of lambs finished were slaughtered 4-8 days after CT scanning (n = 217), The remaining lambs were slaughtered 32-33 days after CT scanning (n = 160), to allow taste panel analysis after a 30 day withdrawal period from the CT sedative, which formed part of the wider study. Carcasses were subjected to high voltage electrical stimulation, chilled for between 7-9 days and dissected, removing muscles from the right side of the carcass at the loin (*M. Longissimus lumborum*), which were vacuum-packed and frozen. The muscle samples were transported to the University of Bristol for MQ analyses, chemical IMF was measured

in a cross-sectional sample taken from the cranial end of the *M. longissimus lumborum* (at the first lumbar vertebra). Each sample was blended to a fine paste and chemical IMF percentage was measured using petroleum ether (B.P. 40-60^{o}C) as the solvent in a modified Soxhlet extraction.

3. Statistical analyses

Prior to any statistical analysis, animals included in the data set without full CT information were removed (n = 2), animals with no IMF data were removed (n = 2), and finally obvious outliers were identified and animals with chemically-extracted IMF percentages identified as outliers were removed from the data set (n = 3).

CT traits tested in the models to explain variation in IMF included carcass fat predicted using the prediction equation above (PR_CFAT), as well as measurements from the segmented carcass portions of the three CT reference scan sites (ISC, LV5 and TV8): muscle area (MA); fat area (FA); average muscle density (MD); average fat density (FD); standard deviation of muscle density (MSD); standard deviation of fat density (FSD); average soft tissue density (STD); and the standard deviation of soft tissue density (STSD). The meat quality trait measured was chemically-extracted intramuscular fat content (IMF_Loin) measured in the loin muscle (*M. longissimus lumborum*). Number of days from CT to slaughter (group 1: 4 to 8 days; group 2: 32 to 33 days to account for those CT scanned early to allow subsequent taste panel analyses) showed no significant effect on IMF levels and was therefore not included in the final statistical analyses.

Mean IMF was 1.48% (s.d. 0.68) and ranged from 0.27 – 3.88%. The distribution of IMF is shown in figure 3 and a summary of the CT and MQ traits can be found in Table 1.

Phenotypic correlations amongst CT variables and chemically extracted IMF in the loin were calculated to identify linear relationships between variables (Table 2). Given the strong phenotypic relationship between predicted carcass fat (PR_CFAT) and chemically extracted IMF in the loin (IMF_Loin), predicted carcass fat was fitted as a prefix predictor variable (indicative for a 'base line') in all models. Statistical analyses used simple, multiple and generalized stepwise linear regression in Genstat 14 (Payne, Murray, Harding, Baird & Soutar, 2012; Payne et al., 2012). Subsequent models added CT measurement traits in a progressive manner. Firstly, CT parameters from all three reference scan images, including the novel 'soft tissue' calculation (combining the density ranges between fat

and muscle), were used to produce prediction equations for IMF. Following this, information from the LV5 scan only was used.

To investigate whether prediction accuracies of IMF_Loin could be increased by focusing on the areas of the CT images from which IMF was actually measured, further virtual dissection analysis (segmenting regions of interest from the saved CT images) was then considered. This involved selecting a subset of animals from the EXP 1 trial (n=100 from year 2003). Mean IMF was 1.77% (SD = 0.72), ranging from 0.42% to 3.75%. A summary of MQ and CT traits for the subset data employed in the virtual dissection analysis can be found in Table 3.

Sixteen models were tested in the analysis (Table 4). Models using reference data with more than two variables were analysed using stepwise linear regression (Genstat 14^{TM}) to optimise the combination of predictor traits from the maximum model. Models with one or two variables included were analysed using simple or multiple linear regressions, respectively.

Models were then tested for significant differences using their correlation coefficient ($\sqrt{\text{Adj } R^2}$) and applying Fisher's Z transformation (Rasch, Herrendörfer, Bock & Busch, 1978). To make final model selections between those that predicted IMF similarly across the whole data set, cross validation analyses were performed. Available data were split using a natural time series separation in the data (Snee, 1977). EXP1 (2003-2004, n=236) data was used as the training data set, and EXP2 (2009, n=134) data was used as the validation data set. Summary statistics for CT measured traits and MQ traits for both training and validation data sets can be found in Table 6. The fitted terms in the best models derived from the regression analyses of the entire data set were used to produce prediction equations derived using the training data set. These equations were then used to predict the IMF values of animals included in the validation data. The coefficient of determination (R^2) and error of prediction (RMSEP) were calculated for the predicted IMF percentage in the loin against chemically extracted IMF_Loin to identify the simplest and most reliable single model or group of models.

4. Results

4.1. Predicting IMF using reference scan information

As expected, Pr_Cfat alone accounted for a moderate amount of the variation in IMF (Adj R^2 = 0.51, where Adj R^2 = 1- (*Residual MS*/ *Total MS*), the *Total MS* is the sample variance and the *residual MS* is an estimate of σ^2, the variance of a value of Y given the set of X's. The resulting statistic is less biased than R^2, and a better measure to use when comparing models with different numbers of predictors.)

There were ten models, from the fifteen models tested that included additional CT variables, with statistically significant improvement in accuracy of prediction when compared to Pr_Cfat as a single predictor ($p<0.05$). Models C^{ref}, D^{ref}, E^{ref}, G^{ref} and I^{ref} were shown not to be significantly different in prediction accuracy from Pr_Cfat (A^{ref}) (Adj R^2 = 0.54, 0.60, 0.57, 0.60 and 0.56, respectively). All other models were >Adj R^2 = 0.63 (Table 4).

From these ten models, the model with the highest Adj R^2 value was identified (model L^{ref}; Adj R^2 = 0.68), which included areas, densities and density standard deviations for both fat and muscle in the maximum model. The fitted terms included muscle density from the LV5 and TV8 scans, fat density from the LV5 scan, muscle area from the ISC scan and fat area from the LV5 and TV8 scans. This model was then used as a benchmark model in order to compare the ten models identified as better predictors of IMF from reference scan information than Pr_Cfat alone.

Models with statistically significantly lower accuracy compared to the benchmark model (L^{ref}) ($p<0.05$) were discarded. All ten original models identified were retained, however the final fitted terms in models B^{ref} and H^{ref} were identical following the stepwise procedure, and as a result model H^{ref} was discarded. This left nine models (including the benchmark model L^{ref}) with correlation coefficients that were not significantly different from one another, meaning that the prediction ability of these nine models is statistically similar. Therefore, a group of models was identified that would equally well predict IMF using different combinations of reference scan information. These models included M^{ref} (Adj R^2 0.64), B^{ref} (Adj R^2 0.66), F^{ref}, J^{ref}, K^{ref} (Adj R^2 0.67), L^{ref}, N^{ref}, O^{ref}, P^{ref} (Adj R^2 0.68).

4.2. Predicting IMF using LV5 scan information

Models using only information from the LV5 scan image were again compared to the simple linear model using only PR_CFAT and nine models were identified as being significantly more accurate in

the prediction of IMF. These models were B^{LV5}, F^{LV5} (Adj R^2 0.63), H^{LV5}, J^{LV5}, N^{LV5}, O^{LV5} (Adj R^2 0.64), K^{LV5}, P^{LV5} (R^2 0.65) and L^{LV5} (Adj R^2 0.66).

Model B^{LV5} and F^{LV5} resulted in the same final fitted terms following the stepwise procedure, so F^{LV5} was discarded, leaving eight final models shown not to be significantly different from the benchmark model (L^{ref}) ($p<0.05$). These eight models were then tested for significance against the model including the largest amount of explanatory variables from the group of models identified as most accurate in explaining the variation of IMF_Loin (Model L^{ref}) in the entire data set. All eight models were retained, as none were shown to be significantly different from model L^{ref} ($p<0.05$)

4.3. Predicting IMF using virtually dissected images from a single LV5 scan

Image analysis then considered the use of regions of interest (ROI) taken from the LV5 scan, comparing the use of information from: (i) the full LV5 scan (LV5); (ii) Dissect[1]; or (iii) Dissect[2] (Figure 2). Models were again compared using the correlation coefficient of each model and tested for significant differences using Fisher's Z transformation.

There was no significant improvement in accuracy at any stage during the virtual dissection of the LV5 image, and in many cases there was a decrease in accuracy, compared to using data from the full LV5 image, although again not a significant decrease (Table 5). Furthermore, there was no significant improvement in the accuracy of the models within method employing additional information from CT variables.

4.4. Model validation and selection

These analyses identified seventeen models that were shown to be statistically similar in their prediction accuracies of IMF_Loin, including either information from the reference scans or LV5 scan only.

The final seventeen models identified were then used to perform cross validation analysis. Seventeen prediction equations were derived using the training data set, corresponding to the seventeen 'best' models identified from primary analysis (Table 7). The models were then used to predict the IMF values of animals included in the validation data. Coefficients of determination (R^2) and error of prediction (RMSEP) for the predicted IMF percentage in the loin against chemically extracted IMF_Loin are also shown in Table 7.

The models with the strongest cross validity were models M^{ref} (R^2_{cal} = 0.64, R^2_{val} = 0.67) and N^{ref} (R^2_{cal} = 0.67, R^2_{val} = 0.67), using soft tissue density information from all three reference scans (M^{ref}) and using soft tissue density information from the LV5 and TV8 scans alongside the standard deviation of soft tissue density from all three reference scans (N^{ref}). Residual mean square error of prediction (RMSEP) in the validation data compared to the calibration data, decreased slightly across all models. The reduction of RMSEP is due to the characteristics of the validation data set (Figure 3). The reduction in variation of IMF across the validation data set reduces the error of the prediction. These models were then used as a benchmark and all other models were tested for significant differences in correlation coefficients using Fisher's z transformation (Rasch et al., 1978). All seventeen models were found to be statistically similar in prediction accuracy ($p<0.05$) and no significant reduction in prediction accuracy was seen across the calibration and validation models. From this, two models were chosen from the criteria of firstly, the simplest and best model (N^{ref}) and the simplest model that was shown to be significantly more accurate in prediction than the baseline (B^{ref}). Final models are shown below.

$Pr\_IMF\_B^{ref}$ (%) = 6.920 + (Pr_Cfat*0.2425) - (LV5MD*0.0654) – (TV8MD*0.0637)

$Pr\_IMF\_N^{ref}$ (%) = 7.320 + (Pr_Cfat*0.0565) – (LV5STD*0.0626) – (TV8STD*0.03585) + (ISCSTSD*0.02209) – (LV5STSD*0.0565) – (TV8STSD*0.0303)

5. Discussion

A minimum level of 3% chemically extracted intramuscular fat in grilled cuts of lamb, ensuring consumer acceptability, was recommended following a review of the literature by Savell and Cross (1988). During this study the mean IMF% reported for purebred Texel was 1.48%, well below the level recommended by Savell and Cross. At a similar end point mean IMF% in Scottish Blackface lambs was reported as 2.28% (Lambe et al., 2008). In a separate study involving crossbred lambs from several Terminal, Maternal and Merino sires mean IMF% was 4.1% in females and 4.2% in males. And mean IMF% values of 4.3%, 4.5% and 4.1% in lambs from the Maternal, Merino and Terminal sires respectively (Pannier et al., 2014), providing evidence of breed differences when considering IMF levels in sheep.

It has been shown in previous studies that muscle density information from single or multiple CT scans taken along the body of sheep *in vivo* can provide moderately accurate predictions of IMF contained within *M. longissimus* of different sheep breeds at finishing. Published prediction accuracies include $R^2 = 0.33$ using muscle density information from reference scan images in Scottish Blackface sheep (Karamichou et al., 2006), $R^2 = 0.36$ employing information from a cross-sectional scan in the 5th lumbar vertebra of purebred Texel sheep (only using muscle density) and in the same study a reasonable improvement in accuracy was shown when fat density and standard deviations of both fat and muscle density were added to the model ($R^2 = 0.48$) (Lambe et al., 2010). Macfarlane et al. (2005) used similar lean tissue measurements, alongside fat area measurements, in a single cross-sectional scan at the 2nd lumbar vertebra, resulting in a moderate prediction accuracy of $R^2 = 0.57$. These previous studies have shown the possibilities of using CT scanning as a predictor of IMF in different sheep breeds.

This current study did not fully investigate the effect that other fat deposits, such as intrafibre lipid, within the muscle cell may have on CT measured muscle density. Also that the chemical extraction method used to measure IMF% was not sufficient to provide such information.

The use of different statistical approaches, such as partial least squares (PLS) regression compared to ordinary least squares (OLS) regression, has also been investigated in the prediction of IMF in pig loins (*post-mortem* and *in vivo*), alongside the use of combinations of different x-ray intensities and slice thicknesses. These methods, applied *post-mortem*, have achieved prediction accuracies ranging from $R^2 = 0.63$-0.80 (Font-i-Furnols, Brun, Tous & Gispert, 2013). A similar approach *in vivo* achieved maximum prediction accuracies of $R^2 = 0.53$, with poor results during validation of the models (maximum $R^2 = 0.18$) (Kongsro & Gjerlaug-Enger, 2013).

The methods chosen for the statistics (PLS) and x-ray CT intensities aim to deal with the partial volume effect of mixed pixels (pixels consisting of a mixture of fat and muscle), when considering IMF. For example, different x-ray intensities can change the contrast observed between soft tissues. In terms of statistical treatment of the data, the PLS approach considers the proportion of pixels allocated to each HU value, whereas OLS employs information across a range of HU values within defined thresholds. Font-i-Furnols *et al.* (2013) found that the estimation of IMF in pork loins post mortem is

better predicted by OLR than PLS regression, and that a reduced x-ray intensity (increasing contrast) was more accurate, however combining information from high and low intensity improved the prediction accuracy further.

There may be scope for very complex approaches to explain the variation in IMF using CT data. However, this study provides evidence that the use of relatively simple means and standard deviations of the CT parameters routinely captured can be used to predict IMF in the loin of Texel sheep with moderately high accuracy.

The results from this study also show that further improvements are possible in the prediction of intramuscular fat *in vivo* compared to results from similar previous studies (Karamichou et al., 2006; Lambe et al., 2010; Macfarlane et al., 2005), with the use of additional information from multiple cross sectional reference scans. These results show that muscle density is a good predictor of intramuscular fat, agreeing with previous literature sources, and the strong phenotypic relationship between CT predicted carcass fat and intramuscular fat provides some improvement in the accuracy of prediction over that of CT muscle density parameters alone. In this study the addition of standard deviation of muscle density did not significantly improve the accuracy of prediction, as it did in previous studies (Lambe et al., 2010). The inclusion of soft tissue density standard deviation resulted in a slight increase in accuracy. The biological relationship between the standard deviation of soft tissue density and intramuscular fat is not fully understood and requires further analysis. It appears that the distribution of muscle and fat pixels changes and the proportion of 'mixed' pixels (pixels containing both fat and muscle density values according to thresholds) within the soft tissue distributions increases in animals with higher levels of IMF. This equates to an increase in mixed pixels with average density values closer to fat thresholds, indicating that they may contain an increased proportion of fat within the pixel area, reducing the average density value within the pixel, although the overall density remains within the muscle thresholds. There is a possibility that the standard deviation of muscle, fat or soft tissue may also produce some clarity in the models when dealing with the partial volume effect mentioned previously.

The inclusion of CT-predicted carcass fat understandably increases the accuracy of prediction when included in the model and was specifically chosen as a prefix to models and initial benchmark as a

single predictor variable due to the strong phenotypic relationship between CT predicted carcass fat and chemically extracted intramuscular fat (r = 0.71). An increase in accuracy of prediction of IMF from additional parameters, above that provided by Pr_Cfat, is necessary to enable selection for IMF while maintaining or further reducing overall carcass fat. Including both carcass fat and IMF predictors as selection criteria in a multi-trait selection index would then allow simultaneous selection for each fat trait in opposite directions.

The virtual dissection, and use of information from a defined ROI of the loin, did not improve the accuracy of prediction. This intuitive approach to analyse closer to the area from which chemical IMF was measured proved unsuccessful and suggests that there is valuable muscle and fat density information within the carcass portion of the scan images from other muscles, muscle groups and fat depots that provides an increase in accuracy. This may be further acknowledged given the prediction ability of carcass fat information (Pr_Cfat).

The results from this study show that there may be several possible models that have the potential to be used in the prediction of IMF in the loin, indicating a possible ceiling in the prediction accuracy of models employing CT parameters included in this study. Choosing between such a group of models proves difficult. However a choice may be made when considering the best model; employing information on soft tissue density and its standard deviation (N^{ref}, Adj R^2 = 0.68), and the simplest model that was not significantly different in accuracy; employing muscle density information from two of the three reference scan sites (B^{ref}, Adj R^2 = 0.66), with the inclusion of CT-predicted carcass fat in both cases.

This enables us to predict IMF in sheep with the best accuracy using a vast amount of historic CT data obtained at SRUC's CT unit over the last 15 years, providing powerful data sets to estimate heritabilities for CT-predicted IMF and genetic correlations to other production traits. Estimation of these genetic parameters is a required pre-requisite for the integration of this new trait into breeding programmes. Existing studies involving different sheep breeds (Lorentzen & Vangen, 2011) have reported moderate heritabilities of IMF in Norwegian white crossed with Texel terminal sires (h^2 = 0.48, s.e. = 0.16), suggesting that selection for increased IMF should be successful.

These further studies of the genetic parameters will consider the genetic correlations between models including Pr_Cfat and models not including Pr_Cfat.

Further investigations into the application of CT measurements in the prediction of IMF across other sheep breeds is also required to determine whether across-breed prediction equations would be applicable or breed-specific prediction equations would require development, given that the breed used in this study (Texel) were particularly lean and other breeds may be higher in average IMF levels with greater variation.

6. Conclusion

The prediction of IMF in the loin of purebred Texel sheep is possible using information on muscle density from one single scan across the loin region of the animal, alongside CT-predicted total carcass fat. The accuracy of prediction can be further increased employing information from additional anatomical scans, and by also considering fat density and standard deviations of tissue density values, although these increases in accuracy are not always significant. Some of the more complex models including information related to the soft tissue parameters (combining muscle and fat) appear to be more robust at predicting IMF across different populations. This method may now be applied to a powerful dataset to estimate genetic parameters, allowing judgment of how to improve IMF genetically without compromising important production traits including carcass quality.

References

Bunger, L., Macfarlane, J. M., Lambe, N. R., Conington, J., McLean, K. A., Moore, K., Glasbey, C. A., & Simm, G. (2011). Use of X-Ray Computed Tomography (CT) in UK Sheep Production and Breeding. In S. Karuppasamy, *CT Scanning - Techniques and Applications* (pp. 329-348).

Font-i-Furnols, M., Brun, A., Tous, N., & Gispert, M. (2013). Use of linear regression and partial least square regression to predict intramuscular fat of pig loin computed tomography images. *Chemometrics and Intelligent Laboratory Systems,* (122), 58-64.

Glasbey, C. A. & Young, M. J. (2002). Maximum a Posteriori Estimation of Image Boundaries by Dynamic Programming. *Journal of the Royal Statistical Society. Series C (Applied Statistics), 51* (2), 209-221.

Kalender, W. A. (2005). *Computed Tomography: Fundamentals, System technology, Image quality, Applications*. ed 2nd revised. Publicis corporate publishing.

Karamichou, E., Richardson, R. I., Nute, G. R., Mclean, K. A., & Bishop, S. C. (2006). Genetic analyses of carcass composition, as assessed by X-ray computer tomography, and meat quality traits in Scottish Blackface sheep. *Animal Science, 82* , 151-162.

Kongsro, J. & Gjerlaug-Enger, E. (2013). In vivo prediction if intramuscular fat in pigs using computed tomography. *Open Journal of Animal Sciences, 3* (4), 321-325.

Lambe, N. R., McLean, K. A., Macfarlane, J. M., Johnson, P. L., Jopson, N. B., Haresign, W., Richardson, R. I., & Bunger, L. (2010). Predicting intramuscular fat content of lamb loin fillets using CT scanning. *Proceedings of the Farm Animal Imaging Congress*.

Lambe, N. R., Navajas, E. A., Schofield, C. P., Fisher, A. V., Simm, G., Roehe, R., & Bunger, L. (2008). The use of various live animal measurements to predict carcass and meat quality in two divergent lamb breeds. *Meat Science, 80* (4), 1138-1149.

Lambe, N. R., Richardson, R. I., Macfarlane, J. M., Nevison, I., Haresign, W., Matika, O., & Bunger, L. (2011). Genotypic effects of the Texel Muscling QTL (TM-QTL) on meat quality in purebred Texel lambs. *Meat Science, 89* (2), 125-132.

Lorentzen, T. K. & Vangen, O. (2011). Genetic and phenotypic analysis of meat quality traits in lamb and correlations to carcass composition. *Livestock Science, 143* , 201-209.

Macfarlane, J. M., Lewis, R. M., Emmans, G. C., Young, M. J., & Simm, G. (2006). Predicting carcass composition of terminal sire sheep using X-ray computed tomography. *Animal Science, 82* (03), 289-300.

Macfarlane, J. M., Young, M. J., Lewis, R. M., Emmans, G. C., & Simm, G. (2005) Using X-ray computed tomography to predict intramuscular fat content in terminal sire sheep. *56th Annual Meeting of the European Association for Animal Production*, 264.

Mann, A. D., Young, M. J., Glasbey, C. A., & McLean, K. A. (2003). STAR:Sheep Tomogram Analysis Routines (V.3.4). *BioSS software documentation*.

Moore, K., McLean, K. A., & Bunger, L. (2011). The benefits of Computed Tomography (CT) scanning in UK sheep flocks for improving carcase composition. *Proceedings of the British Society of Animal Science and the Association of Veterinary Teaching and Research Work, 2* (1), 10.

Pannier, L., Pethick, D. W., Geesink, G. H., Ball, A. J., Jacob, R. H., & Gardner, G. E. (2014). Intramuscular fat in the longissimus muscle is reduced in lambs from sires selected for leanness. *Meat Science, 96* (2, Part B), 1068-1075.

Payne, R., Murray, D., Harding, S., Baird, D., & Soutar, D. (2012). *Introduction to Genstat for Windows*. ed 15. VSN International.

Rasch, D., Herrendörfer, G., Bock, J., & Busch, K. (1978). *Verfahrensbibliothek Versuchsplanung und -auswertung - Band 1*. Berlin: VEB Deutscher Landwirtschaftsverlag.

Savell, J. W. & Cross, H. R. (1988). The role of fat in the palatability of beef, pork and lamb. In Anonymous, *Designing foods: Animal product options in the marketplace* (pp. 345-355). National Academy Press.

Smith, G. C. & Carpenter, Z. L. (1974). Eating quality of meat animal products and their fat content. *Fat content and composition of animal products: Proceedings of a symposium,* 147-182.

Snee, R. D. (1977). Validation of Regression Models: Methods and Examples. *Technometrics, 19* (4), 415-428.

Sonesson, A. K., de Greef, K. H., & Meuwissen, T. H. E. (1998). Genetic parameters and trends of meat quality, carcass composition and performance traits in two selected lines of large white pigs. *Livestock Production Science, 57* (1), 23-32.

Young, M. J., Simm, G., & Glasbey, C. A. (2001). Computerised tomography for carcass analysis. *Proceedings of the British Society of Animal Science,* 250-254.

Figure 1 Topogram and 2D cross sectional CT scans at the ischium (i), 5th lumbar vertebra (ii) and 8th thoracic vertebra (iii)

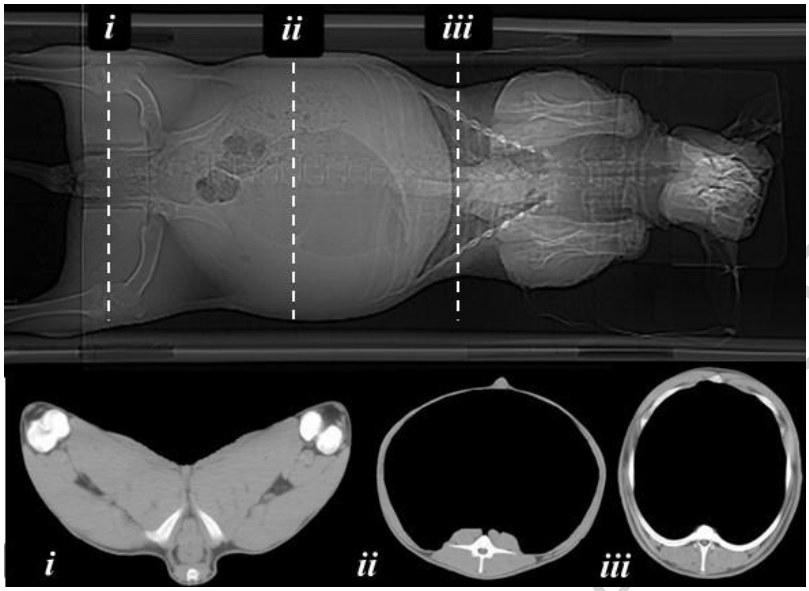

Figure 2 Virtual dissection of LV5 scan, LV5 only (i), Dissect1 (ii) and Dissect2 (iii)

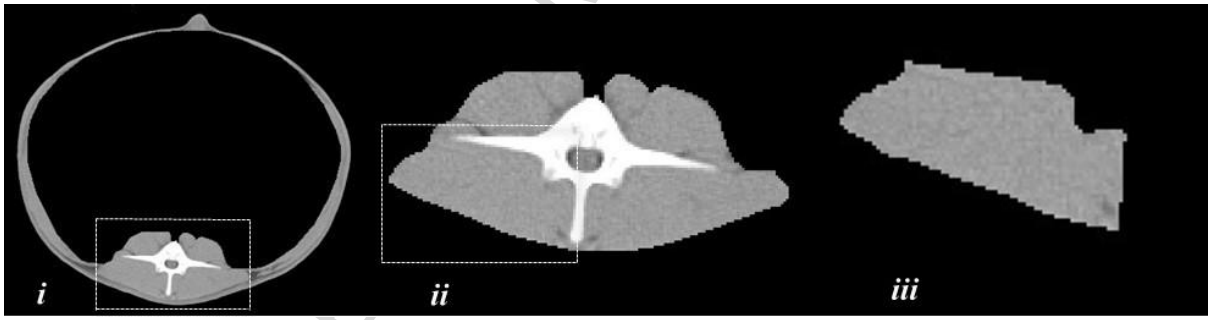

Table 1 Trait descriptions, means and standard deviations (SD) (n=370)

Trait	Acronym	Trait Description	Mean	SD
CT Traits				
	ISCMD	Average muscle density at ischium scan site (HU)	48.44	2.10
	ISCMSD	Standard deviation of muscle density at ischium scan site (HU)	16.81	0.81
	ISCFD	Average fat density at ischium scan site (HU)	-62.37	5.32
	ISCFSD	Standard deviation of fat density at ischium scan site (HU)	36.51	2.50
	ISCFA	Carcass fat area measured at ischium scan site (mm^2)	3651	1404
	ISCMA	Muscle area measured at ischium scan site (mm^2)	27415	2898
	LV5MD	Average muscle density at 5^{th} lumbar vertebra scan site (HU)	48.30	2.65
	LV5MSD	Standard deviation of muscle density at 5^{th} lumbar vertebra scan site (HU)	18.47	1.67
	LV5FD	Average fat density at 5^{th} lumbar vertebra scan site (HU)	-66.41	7.20
	LV5FSD	Standard deviation of fat density at 5^{th} lumbar vertebra scan site (HU)	42.68	4.35
	LV5FA	Carcass fat area measured at 5^{th} lumbar vertebra scan site (mm^2)	1242	875
	LV5MA	Muscle area measured at 5^{th} lumbar vertebra scan site (mm^2)	9684	1472
	TV8MD	Average muscle density at 8^{th} thoracic vertebra scan site (HU)	44.68	2.98
	TV8MSD	Standard deviation of muscle density at 8^{th} thoracic vertebra scan site (HU)	21.94	1.73
	TV8FD	Average fat density at 8^{th} thoracic vertebra scan site (HU)	-64.64	5.99
	TV8FSD	Standard deviation of fat density at 8^{th} thoracic vertebra scan site (HU)	39.21	3.16
	TV8FA	Carcass fat area measured at 8^{th} thoracic vertebra scan site (mm^2)	3451	1843
	TV8MA	Muscle area measured at 8^{th} thoracic vertebra scan site (mm^2)	12380	1833
	LV5STD	Average soft tissue density at 5^{th} lumbar vertebra scan site (HU)	36.22	8.09
	LV5STSD	Standard deviation of soft tissue density at 5^{th} lumbar vertebra scan site (HU)	40.33	6.19
	ISCSTD	Average soft tissue density at ischium scan site (HU)	35.55	5.07
	ISCSTSD	Standard deviation of soft tissue density at ischium scan site (HU)	40.34	5.66
	TV8STD	Average soft tissue density at 8^{th} thoracic vertebra scan site (HU)	21.84	11.35
	TV8STSD	Standard deviation of soft tissue density at 8^{th} thoracic vertebra scan site (HU)	50.56	6.70
	PR_CFAT	Predicted total carcass fat weight (kg)	2.34	1.11
MQ Traits				
	IMF_Loin	*M. longissimus lumborum* intra-muscular fat (%)	1.48	0.68

Table 2 Phenotypic correlations amongst CT predictor variables in the reference scans and IMF

	IMF_LOIN	PR_CFAT	ISCMD	ISCMSD	ISCFD	ISCFSD	ISCFA	ISCMA	ISCSTD
IMF_Loin	-								
PR_CFAT	0.71	-							
ISCMD	-0.28		-						
ISCMSD	0.54	0.68		-					
ISCFD	-0.38	-0.50	-0.18	-0.11	-				
ISCFSD	-0.48	-0.64		-0.50		-			
ISCFA	0.72	0.93		0.68	-0.60	-0.63	-		
ISCMA	0.20	0.63	0.33	0.46		-0.47	0.42	-	
ISCSTD	-0.74	-0.72	0.47	-0.56	0.55	0.48	-0.86		-
ISCSTSD	0.68	0.81		0.58	-0.75	-0.48	0.93	0.22	-0.87
	IMF_LOIN	PR_CFAT	LV5MD	LV5MSD	LV5FD	LV5FSD	LV5FA	LV5MA	LV5STD
LV5MD	-0.71	-0.59	-						
LV5MSD	0.66	0.68	-0.71	-					
LV5FD	0.47	0.45	-0.58	0.71	-				
LV5FSD	-0.71	-0.83	0.64	-0.79	-0.66	-			
LV5FA	0.71	0.90	-0.61	0.69	0.31	-0.85	-		
LV5MA	0.26	0.64	-0.20	0.23	0.35	-0.39	0.41	-	
LV5STD	-0.76	-0.80	0.77	-0.76	-0.39	0.82	-0.92	-0.23	-
LV5STSD	0.65	0.75	-0.57	0.73	-0.27	-0.79	0.90	0.16	-0.94
	IMF_LOIN	PR_CFAT	TV8MD	TV8MSD	TV8FD	TV8FSD	TV8FA	TV8MA	TV8STD
TV8MD	-0.72	-0.58	-						
TV8MSD	0.24	0.17	-0.25	-					
TV8FD	-0.37	-0.51	0.23		-				
TV8FSD	-0.60	-0.70	0.61	-0.17		-			
TV8FA	0.75	0.92	-0.70	0.30	-0.63	-0.66	-		
TV8MA	0.25	0.60	-0.17	-0.25		-0.48	0.42	-	
TV8STD	-0.76	-0.80	0.80	-0.36	0.60	0.63	-0.93	-0.20	-
TV8STSD	0.65	0.73	-0.61	0.47	-0.68	0.53	0.88	0.12	-0.94

Only correlations greater than zero ($P<0.05$) are shown

Figure 3 Distribution of IMF% in the loin (n=370), Calibration (n=236) and Validation (n=134) data

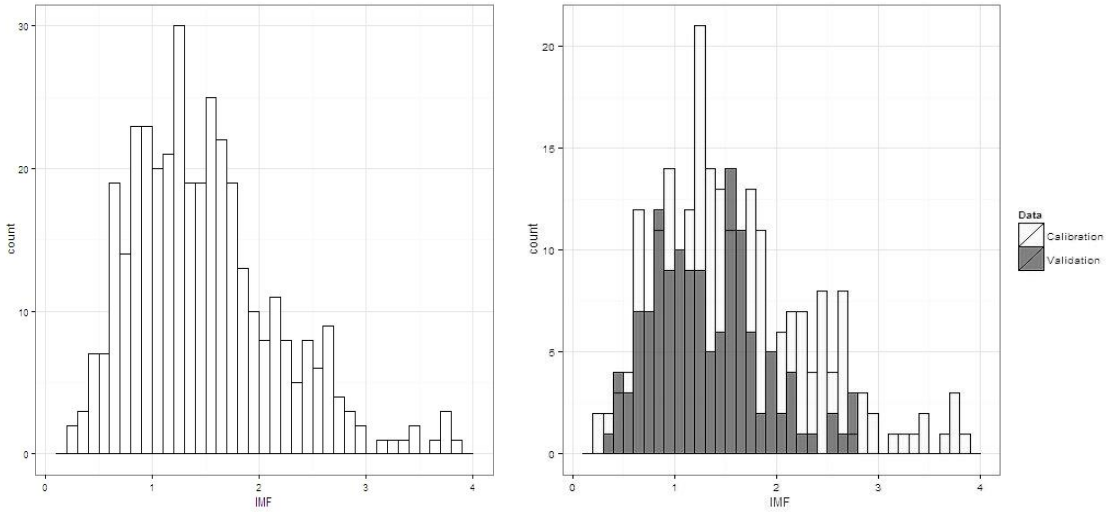

Table 3 CT and MQ traits, means and standard deviations for lambs included in the virtual dissection data set (n=100)

	LV5		Dissect[1]		Dissect[2]	
	Mean	SD	Mean	SD	Mean	SD
MQ Trait						
IMF_Loin	1.77	0.72	1.77	0.72	1.77	0.72
CT Trait						
LV5FD	-63.86	5.81	-37.66	6.84	-28.12	12.18
LV5FSD	41.23	4.36	22.81	5.16	12.04	8.26
LV5MD	47.52	2.26	55.15	1.68	57.2	1.83
LV5MSD	18.83	1.38	13.72	0.81	11.93	0.85
LV5STD	34.13	8.61	54.19	1.92	56.76	2.04
LV5STSD	41.34	6.84	16.72	1.76	13.42	2.08

[LV5] Using information from LV5 only, [1] Using information from dissect[1] CT parameters, [2] Using information from dissect[2] CT parameters

Table 4 Linear regression models between IMF and CT tissue density parameters, with adjusted coefficient of determination (R^2) and residual mean square error (RMSE), based on the whole data set (n=370)

		Ref[1]		LV5[2]	
	Maximum Model	**Adj R^2**	**RMSE**	**Adj R^2**	**RMSE**
A	Pr_Cfat	0.51	0.48	0.51	0.48
B	Pr_Cfat+MD	0.66[ab]	0.40	0.63[ab]	0.41
C	Pr_Cfat+FD	0.54	0.47	0.54	0.47
D	Pr_Cfat+MA	0.60[b]	0.43	0.56	0.45
E	Pr_Cfat+FA	0.57	0.45	0.53	0.47
F	Pr_Cfat+MD+FD	0.67[ab]	0.40	0.63[ab]	0.41
G	Pr_Cfat+MA+FA	0.60[b]	0.43	0.56	0.45
H	Pr_Cfat+MD+MSD	0.66[ab]	0.40	0.64[ab]	0.41
I	Pr_Cfat+FD+FSD	0.56	0.46	0.55	0.46
J	Pr_Cfat+MD+MSD+FD+FSD	0.67[ab]	0.39	0.64[ab]	0.41
K	Pr_Cfat+MD+MSD+FD+FSD+FA	0.67[ab]	0.39	0.65[ab]	0.41
L	Pr_Cfat+MD+MSD+FD+FSD+MA+FA	0.68[ab]	0.39	0.66[ab]	0.40
M	Pr_Cfat+STD	0.64[ab]	0.41	0.60[b]	0.43
N	Pr_Cfat+STD+STSD	0.68[ab]	0.39	0.64[ab]	0.41
O	Pr_Cfat+STD+STSD+FA	0.68[ab]	0.39	0.64[ab]	0.41
P	Pr_Cfat+STD+STSD+FA+MA	0.68[ab]	0.39	0.65[ab]	0.40

[1] Using information from all three reference scans, [2] Using information from LV5 scan only

[a] Adj R^2 values are significantly greater than model A ($p>0.05$)

[b] Adj R^2 values do not differ significantly from model L^{ref} (benchmark)

Table 5 Linear regression models between IMF and CT tissue density parameters during virtual dissection, with adjusted coefficient of determination (R^2) and residual mean square error (RMSE), based on the subset of the data (n=100)

		LV5		Dissect[1]		Dissect[2]	
	Model	**Adj R^2**	**RMSE**	**Adj R^2**	**RMSE**	**Adj R^2**	**RMSE**
A	Pr_Cfat	0.43	0.54	0.43	0.54	0.43	0.54
B	Pr_Cfat+MD	0.61	0.45	0.54	0.49	0.55	0.48
C	Pr_Cfat+FD	0.47	0.52	0.43	0.54	0.44	0.54
D	Pr_Cfat+MA	0.48	0.52	0.49	0.51	0.49	0.51
E	Pr_Cfat+FA	0.44	0.54	0.43	0.54	0.43	0.54
F	Pr_Cfat+MD+FD	0.61	0.45	0.54	0.49	0.58	0.47
G	Pr_Cfat+MA+FA	0.48	0.52	0.49	0.51	0.49	0.51
H	Pr_Cfat+MD+MSD	0.61	0.45	0.54	0.49	0.55	0.48
I	Pr_Cfat+FD+FSD	0.48	0.52	0.45	0.53	0.46	0.53
J	Pr_Cfat+MD+MSD+FD+FSD	0.61	0.44	0.55	0.48	0.59	0.46
K	Pr_Cfat+MD+MSD+FD+FSD+FA	0.61	0.44	0.55	0.48	0.59	0.46
L	Pr_Cfat+MD+MSD+FD+FSD+MA+FA	0.62	0.44	0.57	0.47	0.62	0.44
M	Pr_Cfat+STD	0.54	0.49	0.52	0.50	0.53	0.49
N	Pr_Cfat+STD+STSD	0.56	0.47	0.54	0.48	0.55	0.48
O	Pr_Cfat+STD+STSD+FA	0.60	0.45	0.55	0.48	0.55	0.48
P	Pr_Cfat+STD+STSD+FA+MA	0.61	0.45	0.58	0.47	0.58	0.47

[LV5] Using information from LV5 only, [1] Using information from dissect1 CT parameters, [2] Using information from dissect2 CT parameters

Table 6 CT and MQ traits, means and standard deviations for lambs included in the calibration data set (n=236) and validation data set (n=134)

		Calibration Data (n=236)		Validation Data (n=134)	
Trait	Acronym	Mean	SD	Mean	SD
CT Traits					
	ISCMD	49.32	1.78	46.90	1.69
	ISCMSD	16.87	0.76	16.71	0.89
	ISCFD	-63.48	5.61	-60.43	4.14
	ISCFSD	35.91	1.96	37.57	2.97
	ISCFA	3987	1421	3060	1164
	ISCMA	28318	2492	25823	2887
	LV5MD	48.41	2.62	48.12	2.70
	LV5MSD	18.39	1.67	18.62	1.66
	LV5FD	-65.85	6.61	-67.40	8.07
	LV5FSD	42.26	4.47	43.42	4.03
	LV5FA	1350	982	1051	603
	LV5MA	10160	1319	8846	1350
	TV8MD	44.93	2.97	44.24	2.97
	TV8MSD	21.51	1.68	22.69	1.56
	TV8FD	-64.66	6.57	-64.59	4.84
	TV8FSD	38.50	2.92	40.45	3.18
	TV8FA	3589	1985	3209	1541
	TV8MA	12861	1652	11533	1834
	LV5STD	35.95	8.91	36.71	6.41
	LV5STSD	40.42	6.86	40.17	4.79
	ISCSTD	35.43	5.45	35.77	4.33
	ISCSTSD	41.74	5.89	37.88	4.23
	TV8STD	21.97	12.22	21.62	9.66
	TV8STSD	50.28	7.42	51.06	5.16
	PR_CFAT	2.60	1.08	1.74	1.01
MQ Traits					
	IMF_Loin	1.58	0.74	1.31	0.54

Table 7 Linear regression models between IMF and CT tissue density parameters, with adjusted coefficient of determination (R^2) and residual mean square error (RMSE), based on the training data set (n=236) and validation data set (n=134)

		Calibration (n=236)		Validation (n=134)	
	Fitted Terms	**Adj R^2**	**RMSE**	**Adj R^2**	**RMSEP**
B^{ref}	Pr_Cfat, LV5MD, TV8MD	0.69	0.41	0.63	0.33
F^{ref}	Pr_Cfat, LV5MD, TV8MD, ISCFD	0.69	0.41	0.63	0.33
J^{ref}	Pr_Cfat, LV5MD, TV8MD, ISCFD, LV5FSD	0.69	0.41	0.64	0.32
K^{ref}	Pr_Cfat, LV5MD, TV8MD, ISCFA, LV5FA	0.70	0.41	0.63	0.32
L^{ref}	Pr_Cfat, LV5MD, TV8MD, LV5FD, ISCMA, LV5FA, TV8FA	0.71	0.41	0.65	0.32
M^{ref}	Pr_Cfat, ISCSTD, LV5STD, TV8STD	0.64	0.45	0.67	0.31
N^{ref}	Pr_Cfat, LV5STD, TV8STD, ISCSTSD, LV5STSD, TV8STSD	0.67	0.42	0.67	0.30
O^{ref}	Pr_Cfat, ISCSTD, ISCSTSD, LV5STD, LV5STSD, TV8STD, ISCFA, TV8FA, ISCFA	0.68	0.42	0.66	0.31
P^{ref}	Pr_Cfat, LV5STD, LV5STSD, TV8STD, TV8STSD, ISCMA, TV8FA	0.69	0.41	0.66	0.31
B^{LV5}	Pr_Cfat, LV5MD	0.67	0.43	0.57	0.35
H^{LV5}	Pr_Cfat, LV5MD, LV5MSD	0.67	0.43	0.59	0.35
J^{LV5}	Pr_Cfat, LV5MD, LV5FD, LV5FSD	0.68	0.42	0.57	0.35
K^{LV5}	Pr_Cfat, LV5MD, LV5FSD, LV5FA	0.68	0.42	0.59	0.35
L^{LV5}	Pr_Cfat, LV5MD, LV5FD, LV5MA, LV5FA	0.68	0.42	0.60	0.34
N^{LV5}	Pr_Cfat, LV5STD, LV5STSD	0.64	0.44	0.61	0.34
O^{LV5}	Pr_Cfat, LV5STD, LV5STSD, LV5FA	0.64	0.44	0.61	0.34
P^{LV5}	Pr_Cfat, LV5STD, LV5STSD, LV5MA	0.66	0.43	0.62	0.33